LETTERS
PUBLISHED ONLINE: 4 APRIL 2010 | DOI: 10.1038/NPHYS1630
nature physics

Observation of hidden phases in supersolid ^{4}He

H. Choi, S. Kwon, D. Y. Kim and E. Kim*

Liquid helium becomes a superfluid and flows with zero viscosity at low temperatures. Superfluidity is manifested by a failure to rotate, as its mass is decoupled from the rotation of the containing cell. Supersolid helium should show similar behaviour; apparent rotational inertia decreases when the solid helium is set into torsional oscillation below 200 mK (refs 1,2). However, a number of later experiments[3–7] revealed characteristics unexpected within a conventional superfluid framework. Recent observations include hysteresis in the resonant period[8,9] and relaxation dynamics[10]. To account for the inconsistencies, there are various proposals that include superfluid grain boundaries[11], glassy behaviour[12,13], viscoelasticity[14], a vortex fluid[15] and a superglass[16]. Here we systematically investigate the hysteresis and relaxation processes with a set of temperature and velocity sweeps. We unveil two hidden states associated with pinning of low-temperature excitations and construct a new phase diagram.

Unlike a typical superfluid, the non-classical rotational inertia fraction (NCRIF) has been found to be partially hysteretic[8]. The low-temperature ($T <\sim 20$ mK) value of NCRIF for a sample was smaller when cooled down in a high-velocity field (HVF), versus that obtained at low speeds. On reducing the velocity at the lowest temperature, the NCRIF recovered the unsuppressed value. However, subsequent increases in the velocity did not result in any suppression of the NCRIF up to at least 800 μm s^{-1}. This hysteresis was observed only below about 40 mK. Slow warming and cooling cycles (all below 65 mK) following the above type of velocity sweeps have revealed that the NCRIF can be multivalued at the lowest temperatures[9]. The two research groups involved have described these findings in terms of the pinning of low-temperature excitations (such as dislocations and/or vortices) in solid ^{4}He.

Here we examine the phenomena systematically by measuring the dynamic response of a torsional oscillator containing a bulk ^{4}He sample at a pressure of 40 bar. The sample was grown using the blocked capillary method. The torsional oscillator has an open volume of 1.92 cm^3 in a cylindrical form, with a 13 mm diameter and a height of 14.5 mm. The surface-area to volume (S/V) ratio is 4.46 cm^{-1}. The empty cell has a resonant period of 1.328 ms and a mechanical quality factor of 2×10^6 at 4.2 K.

Two procedures were used to reach a fixed temperature and rim velocity, both of which represent a different history. The first is a typical method from previous studies. After setting the driving voltage at 500 mK, the torsional oscillator was cooled to the base temperature of 23 mK. After equilibration at the lowest temperature, a slow warming scan was carried out. We will refer to this cooling procedure and the corresponding NCRIF as HVF cooling and HVF NCRIF, respectively. As the rim velocity v_R of the torsional oscillator is temperature dependent for a constant driving voltage, we consistently denote each data set by the value of v_R recorded at 23 mK.

The second procedure was as follows. At 500 mK, the driving voltage was set to a low value such that v_R at 23 mK is less than

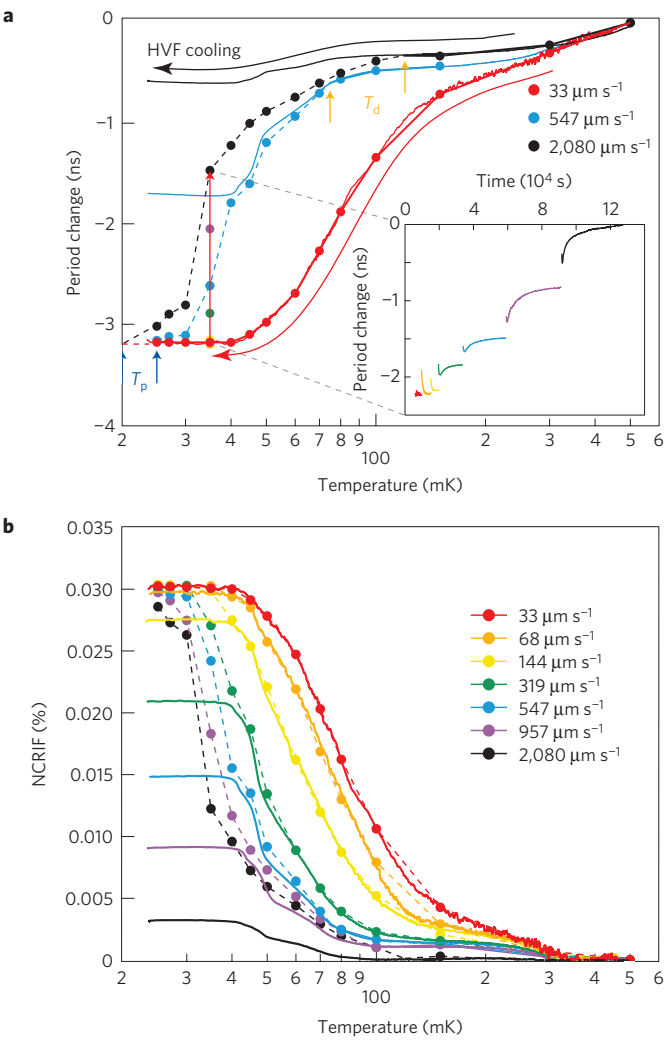

Figure 1 | Period change in a torsional oscillator versus temperature and conversion into NCRIF. a, Two different experimental procedures used in the experiment. The first is HVF cooling (see text). Data are obtained from a subsequent warming scan (solid blue and black curves). The second process involves cooling with $v_R \leq 33$ μm s^{-1} (solid red curve). The rim velocity is increased discretely after the target temperature is reached (solid circles). The inset shows the time evolution of the period on increasing v_R. Colour coded arrows mark T_p and T_d at two different velocities. **b**, NCRIF measured with two different techniques. The dashed curves are guides for the eye.

33 μm s^{-1}. The sample was then cooled down to a particular target temperature. The time evolution of the period and that of the amplitude were subsequently measured as the driving voltage was increased discretely in several steps. When the driving voltage is

Department of Physics and Center for Supersolid & Quantum Matter Research, KAIST, Daejeon 305-701, Republic of Korea. *e-mail: eunseong@kaist.edu.

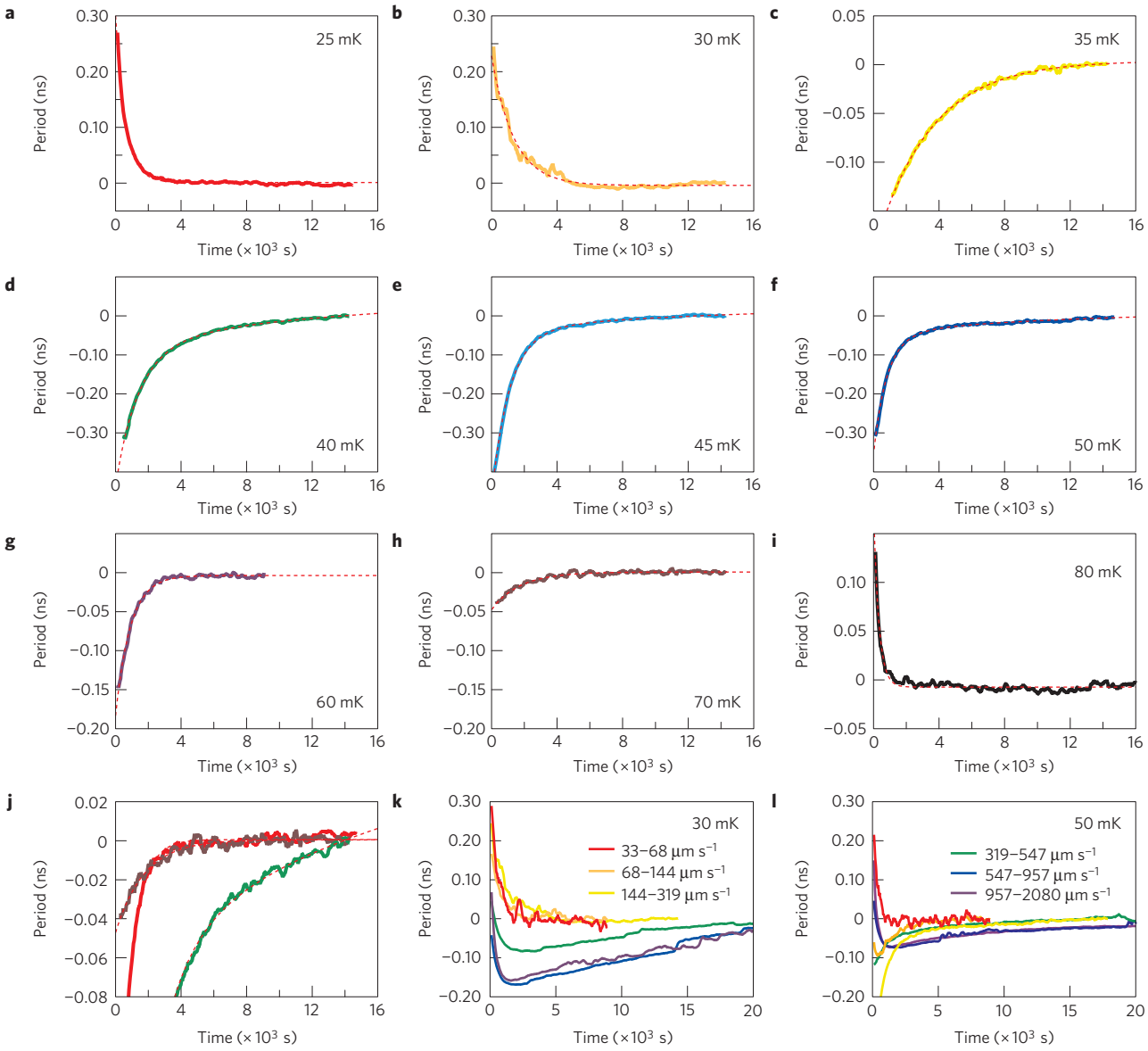

Figure 2 | Dynamic response of a torsional oscillator. a–i, Time evolution of the resonant period, with respect to the equilibrium value, after v_R is increased from 144 to 319 μm s^{-1} at various temperatures. The red dashed curves are fits to data using $P(t) = P_0 + Ae^{-t/\tau} + B\ln(1+t/t_0)$ for **c**–**f** and $P(t) = P_0 + Ae^{-t/\tau}$ for the rest. **j**, Zoom-in of **a**, **d** and **h** to emphasize the change in the relaxation process. The 25 mK data (**a**) have been inverted to fit in the figure. **k**,**l**, Time evolution in response to various rim velocity changes at 30 mK (**k**) and 50 mK (**l**).

stepped up or down there is an abrupt jump—dominated by an instrumental artefact—in the resonant period, followed by slow relaxation. Following each relaxation process, we acquire a value for the NCRIF at the target temperature for each respective rim velocity (see Fig. 1). Owing to the low-velocity field (LVF) cooling to each target temperature, we label each of these traces as LVF NCRIF.

The maximum value of LVF NCRIF observed was 0.03%, which saturated at this value for $T <\sim 35$ mK while cooling with $v_R = 33$ μm s^{-1}. This is one of the smallest reported values so far. Although a quantitatively accurate correlation is not well established, torsional oscillators with small S/V ratios tend to display smaller NCRIF values. This may in part be due to large defect densities near the walls of the cell[17], and also the inefficiency to quickly drain away the latent heat of crystallization so as not to generate thermally induced strains[18].

For HVF cooling, NCRIF at 23 mK is suppressed and projected to disappear at ∼3 mm s^{-1}. Above a specific point that we call the depinning temperature T_d, the HVF and LVF NCRIF values show the same temperature dependence all the way up to the onset temperature T_o. Below T_d, where the two begin to differ, LVF NCRIF is always greater than HVF NCRIF. Moreover, the NCRIF recovers from the HVF value to its unsuppressed value (red curve in Fig. 1b) when the velocity is reduced to 33 μm s^{-1}. This demonstrates that, below T_d, the NCRIF depends on both the temperature and velocity histories of the sample.

We must emphasize that T_d is not simply the temperature at which a difference between HVF and LVF NCRIF emerges, but also the point where the dynamic response of the torsional oscillator changes. Above T_d, the resonant period decays exponentially on a relatively short timescale (see Fig. 2g–j). In contrast, decay takes place much more slowly below T_d (see Fig. 2c–f). Interestingly, at even lower T, below what we define as the pinning temperature T_p, long-timescale characteristics once again disappear (see Fig. 2a and b). We note that T_p also represents the (velocity dependent) temperature above which LVF NCRIF is suppressed. As T_p is below 23 mK for $v_R > 547$ μm s^{-1}, we extrapolated the low-T data to

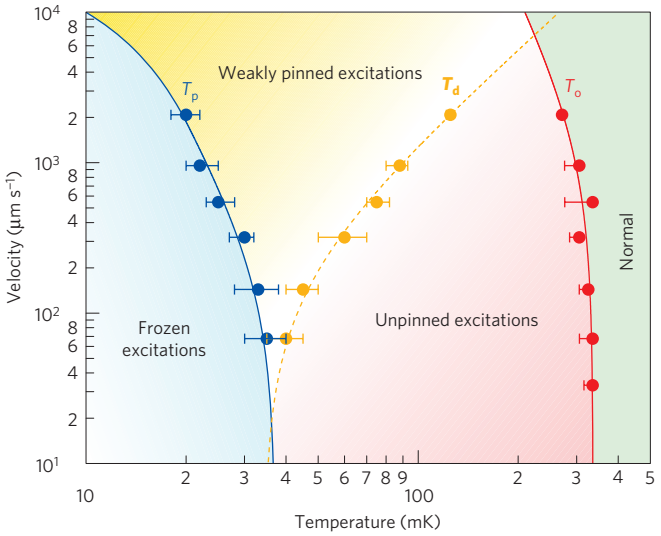

Figure 3 | Velocity–temperature phase diagram of solid ^{4}He obtained by the second procedure described in the text. Above T_o (solid red circles), solid ^{4}He is a normal Debye solid. Below T_o, a fluid of unpinned vortices forms. On a further decrease in temperature, down to $T \approx T_d$ (solid yellow circles), the vortices become weakly pinned. The yellow curve is a fit of the functional form $T_d = C\sqrt{v_R + v_0}$. T_p (filled blue circles) marks the true transitions to a superfluid-like vortex glass at various velocities. The red and blue curves are guides for the eye. The error bars mark uncertainty in transition temperatures determined by the method explained in Supplementary Information Section 2.

estimate the suppression temperature for high velocities (see Fig. 1a and Supplementary Information).

In Fig. 3 we have constructed a phase diagram in the v_R–T plane on the basis of the observed T_p, T_d and T_o. Identification of each phase was possible by analysing the relaxation dynamics of the torsional oscillator. In the red shaded region, the time evolution of the resonant period is exponential. The equilibrium time constant τ is of the order of a few hundred seconds near T_o. This is shorter than that of the empty cell, indicating that there is an extra dissipative process in the solid sample that provides damping to the torsional oscillator. We find that τ increases for $T < 100$ mK, which is consistent with the literature[10,19]. An increase in τ, that is, a slowing down of the internal relaxation of ^{4}He, can be explained by the progressive freezing out of excitations present in the solid[10,20]. The leading candidates for these excitations are dislocations[21,22], vortices and glassy topological defects[12].

In the yellow shaded region between T_p and T_d, the same exponential decay manifested above T_d is present with τ constantly increasing with decreasing temperatures. However, as mentioned earlier, there is a relaxation process that takes place on a different timescale. This behaviour has also been observed in previous works[8,9]. We follow the argument in ref. 8 and fit to a logarithmic time dependence, which is quite successful, as shown in Fig. 2c–f. The logarithmic behaviour could be caused by creep of weakly pinned excitations[23,24]. That is, if the pinned state is metastable in this region, excitations can escape one trapping site and creep to another. As the temperature is reduced, the thermal energy of the excitations will decrease accordingly, allowing them to be weakly pinned on local pinning sites. The pinning of originally free excitations through this mechanism is a continuous process; thus, T_d would not correspond to a thermodynamic phase transition.

Although the type of excitations cannot be directly identified, the velocity dependence of T_d can provide us with some insight. The positive slope of T_d in v_R–T phase space is at first glance counterintuitive. A higher rim velocity adds more kinetic energy to the system so that one would expect a higher probability of depinning (resulting in a negative slope of T_d). However, if the excitations are vortices, the increasing velocity will result in their proliferation and ultimately will yield stronger vortex–vortex interactions. This would give an extra constraint to free-flowing vortices, hence leading to higher depinning temperatures at higher velocities. However, there is no conclusive evidence at this point.

Below T_p, the jump in the resonant period is followed by exponential relaxation, and is similar to that seen in the empty cell. This indicates that the excitations present in solid ^{4}He are no longer metastably pinned, but rather, completely pinned. Such a process would be expected to result from a change in the pinning potential at T_p; that is, the potential is diverging such that excitations can no longer escape. This is different from a gradual crossover from an unpinned to a weakly pinned state, and could possibly be a true phase transition. This is also the region that presents the hysteresis originally observed previously[8]. It is argued that this could be analogous to the Meissner–Ochsenfeld effect in superconductors, implying that T_p is the temperature at which vortices freeze in both position and number. As T_p is velocity dependent, by inverting the relation, the temperature dependence of the velocity at which NCRIF suppression occurs can be obtained. This is the critical velocity $v_c(T)$ of the hidden Meissner–Ochsenfeld-like state. Determining $v_c(0)$ cannot be done accurately owing to the lack of data below 20 mK. Nevertheless, $v_c(0) > 2$ mm s^{-1}, which is much closer to that of superfluid ^{4}He than original estimates[1,2].

Note that $T_p \approx 35$ mK in the zero-velocity limit coincides with the temperature at which NCRIF saturation is observed. Similar behaviour was found in ref. 8, in which they see saturation at ~40 mK (see Fig. 2 in ref. 8). In ref. 10, NCRIF saturation is not achieved even down to 20 mK. Thus, the continuously increasing relaxation time with decreasing temperature that they observed is to be expected. Fig. 3A and B in ref. 10 show that the change in the frequency shift and dissipation both become smaller as T approaches 20 mK, indicating that the time evolution will eventually vanish at a lower temperature (this is also implied in Fig. 3C of their work). The relatively small T_p reported in ref. 10 (the point at which their observed relaxation will disappear) might be related to a rather large NCRIF (4.8%), as opposed to ours (0.03%) or that of ref. 8 (0.1%).

Another type of hysteresis observed in ref. 9 is seen by LVF cooling of the sample, followed by a single-step velocity increase. This will put the solid ^{4}He in the yellow shaded region of our phase diagram. Temperature variation in this region then creates a mixed state between the weakly pinned and HVF-cooled states, resulting in a multivalued NCRIF. Comparison with previous measurements[8–10,19] reveals that despite the variation in the exact values of velocity and temperature, the general features of the phase diagram seem to be universal.

Received 24 September 2009; accepted 26 February 2010; published online 4 April 2010

References

1. Kim, E. & Chan, M. H. W. Probable observation of a supersolid helium phase. *Nature* **427,** 225–227 (2004).
2. Kim, E. & Chan, M. H. W. Observation of superflow in solid helium. *Science* **305,** 1941–1944 (2004).
3. Day, J., Herman, T. & Beamish, J. Freezing and pressure-driven flow of solid helium in vycor. *Phys. Rev. Lett.* **95,** 035301 (2005).
4. Day, J. & Beamish, J. Pressure-driven flow of solid helium. *Phys. Rev. Lett.* **96,** 105304 (2006).
5. Aoki, Y., Kojima, H. & Lin, X. Search for fourth sound propagation in supersolid ^{4}He. *Low Temp. Phys.* **34,** 329–339 (2008).
6. Kim, E. *et al.* Effect of ^{3}He impurities on the nonclassical response to oscillation of solid ^{4}He. *Phys. Rev. Lett.* **100,** 065301 (2008).
7. Kwon, S., Mulders, N. & Kim, E. Absence of slow sound modes in supersolid ^{4}He. *J. Low Temp. Phys.* **158,** 590–595 (2009).

8. Aoki, Y., Graves, J. C. & Kojima, H. Oscillation frequency dependence of nonclassical rotation intertia of solid ^{4}He. *Phys. Rev. Lett.* **99,** 015301 (2007).
9. Clark, A. C., Maynard, J. D. & Chan, M. H. W. Thermal history of solid ^{4}He under oscillation. *Phys. Rev. B* **77,** 184513 (2008).
10. Hunt, B. *et al.* Evidence for a superglass state in solid ^{4}He. *Science* **324,** 632–636 (2009).
11. Pollet, L. *et al.* Superfluidity of grain boundaries in solid ^{4}He. *Phys. Rev. Lett.* **98,** 135301 (2007).
12. Nussinov, Z., Balatsky, A. V., Graf, M. J. & Trugman, S. A. Origin of the decrease in the torsional-oscillator period of solid ^{4}He. *Phys. Rev. B* **76,** 014530 (2007).
13. Andreev, A. F. Supersolidity of glasses. *JETP Lett.* **85,** 585–587 (2007).
14. Yoo, C.-D. & Dorsey, A. T. Theory of viscoelastic behaviour of solid ^{4}He. *Phys. Rev. B* **79,** 100504 (2009).
15. Anderson, P. W. Two new vortex liquids. *Nature Phys.* **3,** 160–162 (2007).
16. Boninsegni, M., Prokof'ev, N. & Svistunov, B. Superglass phase of ^{4}He. *Phys. Rev. Lett.* **96,** 105301 (2006).
17. Rittner, A. S. C. & Reppy, J. D. Probing the upper limit of nonclassical rotational inertia in solid helium 4. *Phys. Rev. Lett.* **101,** 155301 (2008).
18. West, J. T., Lin, X., Cheng, Z. G. & Chan, M. H. W. Supersolid behaviour in confined geometry. *Phys. Rev. Lett.* **102,** 185302 (2009).
19. Aoki, Y., Keiderling, M. C. & Kojima, H. New dissipation relaxation phenomenon in oscillating solid ^{4}He. *Phys. Rev. Lett.* **100,** 215303 (2008).
20. Nemirovskii, S. K., Shimizu, N., Yasuta, Y. & Kubota, M. Vortex fluid relaxation model for torsional oscillation responses of solid ^{4}He. Preprint at http://arXiv.org/abs/0907.0330v2 (2009).
21. Day, J. & Beamish, J. Low-temperature shear modulus changes in solid ^{4}He and connection to supersolidity. *Nature* **450,** 853–856 (2007).
22. West, J. T., Syshchenko, O., Beamish, J. & Chan, M. H. W. Role of shear modulus and statistics in the supersolidity of helium. *Nature Phys.* **5,** 598–601 (2009).
23. Anderson, P. W. Theory of flux creep in hard superconductors. *Phys. Rev. Lett.* **9,** 309–311 (1962).
24. Cottrell, A. H. *Dislocations And Plastic Flow in Crystals* (Clarendon, 1965).

Acknowledgements

We acknowledge support from the National Research Foundation of Korea through the Creative Research Initiatives. We also thank M. H. W. Chan, H. Kojima, A. C. Clark and the members of the Center for Supersolid & Quantum Matter Research for their helpful discussions.

Author contributions

E.K. designed the project and experiments. H.C. carried out most of the experimental work and data analysis. H.C. and E.K. wrote the manuscript. S.K. and D.Y.K. carried out parts of experimental work.

Additional information

The authors declare no competing financial interests. Supplementary information accompanies this paper on www.nature.com/naturephysics. Reprints and permissions information is available online at http://npg.nature.com/reprintsandpermissions. Correspondence and requests for materials should be addressed to E.K.